3 Biotech (2023) 13:261
https://doi.org/10.1007/s13205-023-03683-z

ORIGINAL ARTICLE

Virtual screening of natural ligands from five resources to target *Ralstonia solanacearum* polygalacturonase and endoglucanase

Faegheh Etminani[1] · **Ebrahim Barzegari**[2]

Received: 18 April 2023 / Accepted: 21 June 2023 / Published online: 2 July 2023

Abstract

The present computational study explores novel herbal compounds with potent inhibitory activity against polygalacturonase (PG) and endoglucanase (EG), the extracellular cell wall-degrading enzymes of *Ralstonia solanacearum* causing crops' bacterial wilt. Phytocompounds of *Rosmarinus officinalis* L., *Coriandrum sativum* L., *Ocimum basilicum*, *Cymbopogon citratus,* and *Thymus vulgaris* were first checked to be pharmacokinetically safe and nontoxic. The ligands were then docked to predicted and validated structural models of PG and EG. Molecular dynamic simulations were performed to ensure the dynamic stability of protein–ligand complexes. Carvone and citronellyl acetate were identified to have the best docking energy in binding and inhibiting PG and EG, respectively. In molecular dynamics, root-mean-square deviations of PG-Carvone and EG-Citronellyl acetate complexes indicated the high stability of the ligands in their corresponding cavities. Root-mean-square fluctuations of both proteins indicated unchanged mobility of the binding site residues due to a stable interaction with their ligands. Functional groups on both ligands contributed to the formation of hydrogen bonds with their respective proteins, which were preserved throughout the simulation time. The nonpolar energy component was revealed to significantly contribute to the stability of the docked protein–ligand complexes. Overall, our findings imply the high capability of Carvone and Citronellyl acetate as strong pesticides against the *R. solanacearum*-caused wilt. This study highlighted the potential of natural ligands in controlling the agricultural bacterial infections, as well as the utility of computational screening techniques in discovering appropriate and potent lead compounds.

Keywords Bacterial wilt · Bactericides · Herbal compounds · Molecular modeling

Introduction

Bacterial wilt brought about by *Ralstonia solanacearum* is a considerably devastating disease (Raza et al. 2016) with an uncommonly broad host range. About 450 different plant species within 50 taxonomic families have been reported as hosts for *R. solanacearum* (Cho et al. 2019). Due to its ability to persist in the soil for long periods (Genin and Denny 2012; Grey and Steck 2001), stress resistance (Kong et al. 2014), non-host colonizing, and latent infection (Van Overbeek et al. 2004), the pathogen is typically difficult to eliminate completely. The global cost burden of this type of wilt cannot be easily assessed owing to its geographically broad prevalence and the variety and degree of symptoms presenting on different crop products.

The pathogen colonized on the root surface invades xylem vessels and causes the cell wall to degrade. Large amounts of exopolysaccharides are then produced, which block the water flow. This blocking leads to chlorosis, wilting, and, ultimately, plant death. *R. solanacearum* secretes several cell-wall-degrading enzymes, which are communally important for its colonization as well as its ability to cause wilt (Liu et al. 2005). Enzymes responsible for plant cell wall degradation include three polygalacturonases (PGs), which are important in the hydrolytic degradation of pectic compounds, and endoglucanase (EG), which cleaves cellulose (Schacht et al. 2011).

There is currently a growing interest in using bioactive organic compounds to suppress pathogenic microorganisms (Daferera et al. 2003). This is mainly due to the

✉ Ebrahim Barzegari
e.barzegari@kums.ac.ir

[1] Department of Plant Protection, University of Kurdistan, Sanandaj, Iran

[2] Medical Biology Research Center, Health Technology Institute, Kermanshah University of Medical Sciences, Kermanshah, Iran

demands to ameliorate the disease or pest incidence so as not to affect the consumer's health and the environment. It also helps to address other important challenges, such as resistance to pesticides (Palacio-Bielsa et al. 2009; Singh et al. 2021).

Thyme (*Thymus vulgaris*), which belongs to the worldwide-distributed family Lamiaceae, has been reported to contain volatile constituents beneficial against Gram-positive and Gram-negative bacteria (Reddy et al. 2014). Abd-Elrahim et al. (2022) revealed *T. vulgaris* essential oil to be highly effective against *R. solanacearum* in a concentration-dependent manner. Paret et al. (2010) proved the bactericidal effect of thyme on *R. solanacearum* race 4, which causes wilts on edible ginger and tomato in tropical regions. Hong et al. (2011) indicated that thyme could reduce wilts on moderately resistant cultivars of tomato. The compound carvacrol of *T. vulgaris* was shown in silico to be cytotoxic to bacteria (Alsaraf et al. 2020). Basil (*Ocimum basilicum* L.; Lamiaceae) is another medicinal herb broadly used for its antibacterial properties (Araujo et al. 2016). In a study by Bassolé et al. (2010), the main compounds of *O. basilicum* (including 57% linalool and 19.2% eugenol) demonstrated toxicity against strains of *E. aerogenes*, *E. coli*, *S. aureus*, *L. monocytogenesm*, *E. faecalis*, *S. typhimurium*, and *S. enteric*. Similar effects were observed by Aliye et al (2021) in their molecular docking analysis to test the antibacterial activities of the *Ocimum* constituents against *S. aureus*, *S. typhimurium*, *K. pneumonia*, and *E. coli*. Rosemary (*Rosmarinus officinalis* L.; Lamiaceae) is a common house plant which has been used extensively as a natural antibacterial medicine (Andrade et al. 2018). Extracts from *R. officinalis* have been reported to contain several bioactive compounds with bactericidal activities (Bozin et al. 2007). Coriander (*Coriandrum sativum* L.) is a medicinal plant widely grown in different world regions. Essential oils from coriander seeds and leaves have been reported to have antimicrobial activity against different Gram-positive/negative bacterial species (Lo Cantore et al. 2004). Lemongrass (*Cymbopogon citratus*) is another potential herb with established antimicrobial effects on a diverse range of Gram-negative and Gram-positive bacteria (Schweitzer et al. 2022).

Computer-aided drug design (CADD) represents important progress in ligand screening and drug discovery (Adam 2005; Taylor 2016). To date, this technique has had limited application in the area of molecular design for controlling crop plants' diseases (Pathak et al. 2016; Zhou et al. 2015). The present study aims to investigate the inhibitory effect of natural compounds from *R. officinalis* L., *C. sativum* L., *O. basilicum*, *C. citratus,* and *T. vulgaris* against the PG and EG enzymes of *R. solanacearum* using the in silico CADD approach.

Materials and methods

Phylogenetic analysis

The protein sequences of polygalacturonase (WP_011004131.1) and endoglucanase (WP_028860305.1) of *R. solanacearum* GMI1000 were obtained from NCBI (https://www.ncbi.nlm.nih.gov). ClustalOmega was employed for the multiple alignment of sequences (Thompson et al. 1994). A phylogenetic tree was then constructed in MEGA 6.0 software (Tamura et al. 2013) using the neighbor-joining method (Saitou and Nei 1987) and Kimura's two-parameter distance (Kimura 1980). Bootstraps were computed with 1000 re-samples. Other parameters were kept default.

Prediction of PG and EG protein structures

Modeling of the 3D protein structures of PG and EG of *R. solanacearum* GMI1000 was performed by I-TASSER (https://zhanggroup.org/I-TASSER). This was followed by optimizing the predicted structures by 3Drefine (http://sysbio.rnet.missouri.edu/3Drefine). The models were validated using the Ramachandran plot and visualized in Chimera 1.8. Default options were applied in all cases. Domain annotations were obtained from InterPro (Paysan-Lafosse et al. 2023).

Ligand structure preparation

The initial list of compounds comprised 119 ligands, including 30, 33, 27, 9, and 20 from *C. sativum* L., *C. citratus*, *O. basilicum*, *R. officinalis* L., and *T. vulgaris*, respectively (summed regardless of their shared presence in multiple plants). This was reduced based on physicochemical properties and distribution to select the safe, nontoxic, and widespread ones. The final set of 37 ligands were searched in PubChem (Kim et al. 2020) to obtain their chemical coordinates. The structures were then optimized using Avogadro software (http://avogadro.cc), to create their energetically most stable state to be used in protein–ligand interaction analyses. The molecular mechanics force field MMFF94 run in 500 steps using the steepest descent algorithm was set to apply geometry optimization on the structure of ligands. The algorithm converged when the energy gradient was smaller than 10^{-7} kcal/mol. Python Viewer 1.5 was used for adding polar hydrogens and file format conversions.

Physicochemical properties

To ensure that the phytocompounds will be pharmacologically harmless and nontoxic if consumed by human, their pharmacokinetic and physicochemical properties were examined by using the SwissADME webserver at http://www.swissadme.ch (Daina et al. 2017). Evaluated features included solubility in lipid (Log $P_{o/w}$; octanol/water distribution coefficient) and water (Log S), as well as the ability to inhibit five important cytochrome P450 (CYP) isoforms, including 1A2, 2C19, 2C9, 2D6, and 3A4, as genetic and cellular toxicity factors.

Molecular docking

Molecular docking between the compounds from *R. officinalis* L., *C. sativum* L., *O. basilicum*, *C. citratus,* and *T. vulgaris* with *R. solanacearum* bacterial enzymes PG and EG was performed using Autodock-4.2.6 implemented in MGL-Tools. Using the FT-site tool (Kozakov et al. 2015), the binding site residues of PG were defined to be Gln221, Lys273, Glu278, Ser292, Trp375, Gln398, Asp421, His453, and Tyr481. In the absence of prior reference to support this prediction, localization of this cavity in the middle of PG's parallel β-helix fold and right on the glycoside hydrolase domain, which are common and conserved structural patterns among pectin degrading enzymes, provides an acceptable validation. For EG, residues Trp223, Ala 157, His216, Leu156, Phe172, Ser155, and Leu219 were determined as the active site (Selvam et al. 2017). The Lamarckian genetic algorithm explored the conformational space of the ligands (Morris et al. 2009). Clusters of binding modes were considered as part of docking output analyses to ensure that the highest energy pose was in the largest cluster. Results were analyzed with AutodockTools and LigPlot software (Wallace et al. 1995). Default parameters were used in the implementation of MGL-Tools, AutodockTools and LigPlot.

Molecular dynamic simulation

For each of the two enzymes (PG and EG), the ligand–protein with the strongest binding was chosen for MD simulation study, comparatively with ligand-free proteins. Ligands' docked conformations were submitted to the server ATB-v3.0 to get the ligands' topologies (Malde et al 2011; Stroet et al. 2018). Topologies for proteins were created using the Gromos-54a7 forcefield, as implemented in Gromacs-v.5.1.2 (Pronk et al. 2013). The defined system included ligand–protein complex within the SPC216 water model as the solvent, all contained in a cubic box with a 10 Å distance between the protein and the box edges. To neutralize charges, eight Cl^- ions were added to the boxes containing PG, and five Na^+ ions were added to those containing EG. Energy minimization using steepest descent for a max of 10,000 steps and until the energy gradient was no greater than 1000 kJ/mol/nm. Canonical equilibration in the constant T of 300 K was done for 200 ps, and then isobaric-isothermal equilibration at constant P of 1 atm and constant T of 300 K was run for 200 ps. Temperature coupling involved the velocity rescale algorithm (Bussi et al. 2007), and pressure coupling applied the Parrinello–Rahman method (Martonak et al. 2003). MD simulations were then continued under isobaric-isothermal conditions, running for 50 ns. Data were saved every 10 ps using 2 fs time steps. Long-range electrostatics were treated by particle mesh Ewald algorithm (Darden et al. 1993) with the cut-off distance of 10 Å. LINCS method was applied to constrain all bonds (Hess et al. 1998). The stability of ligands/proteins was evaluated through the analyses of root-mean-square deviation (RMSD), root-mean-square fluctuation (RMSF), and inter-molecular hydrogen bonding arrays occurring in ligand–protein complexes.

Results

Phylogenetic analysis

Phylogenetic trees constructed based on PG and EG protein sequences are shown in Fig. 1. Both proteins show high diversity among *R. solanacearum* strains, as well as remarkable conservation in the main clusters. As can be seen, PG indicated higher diversity than EG, while EG had a higher level of conservation than PG. The close evolutionary distances generally observed in these trees indicate that the two proteins are sufficiently conserved in terms of sequence, structure and function; thus, they might be suitable targets for inhibition to control *R. solanacearum* infections.

Protein structure prediction

The modeled 3D structures of the studied enzymes are illustrated in Fig. 2a,c. The quality of the predicted structures was assessed using the Ramachandran plot (Fig. 2b,d). PG had 83.9, 10.9, and 5.2%, and EG had 72.9, 14.7, and 12.4% residues located in favored, allowed, and outlier regions of the plot, respectively. This shows the high quality of the models to be used in the next steps for the protein–ligand interaction study.

PG contains two types of functional domains in its structure, including a glycoside hydrolase domain (residues 351–513) and three pectin lyase-like domains (residues 138–277, 351–513, and 608–667) that have been shown in Fig. 2a. EG includes a cellulose binding-like domain (residues 159–248) and an RlpA-like domain (residues 48–156;

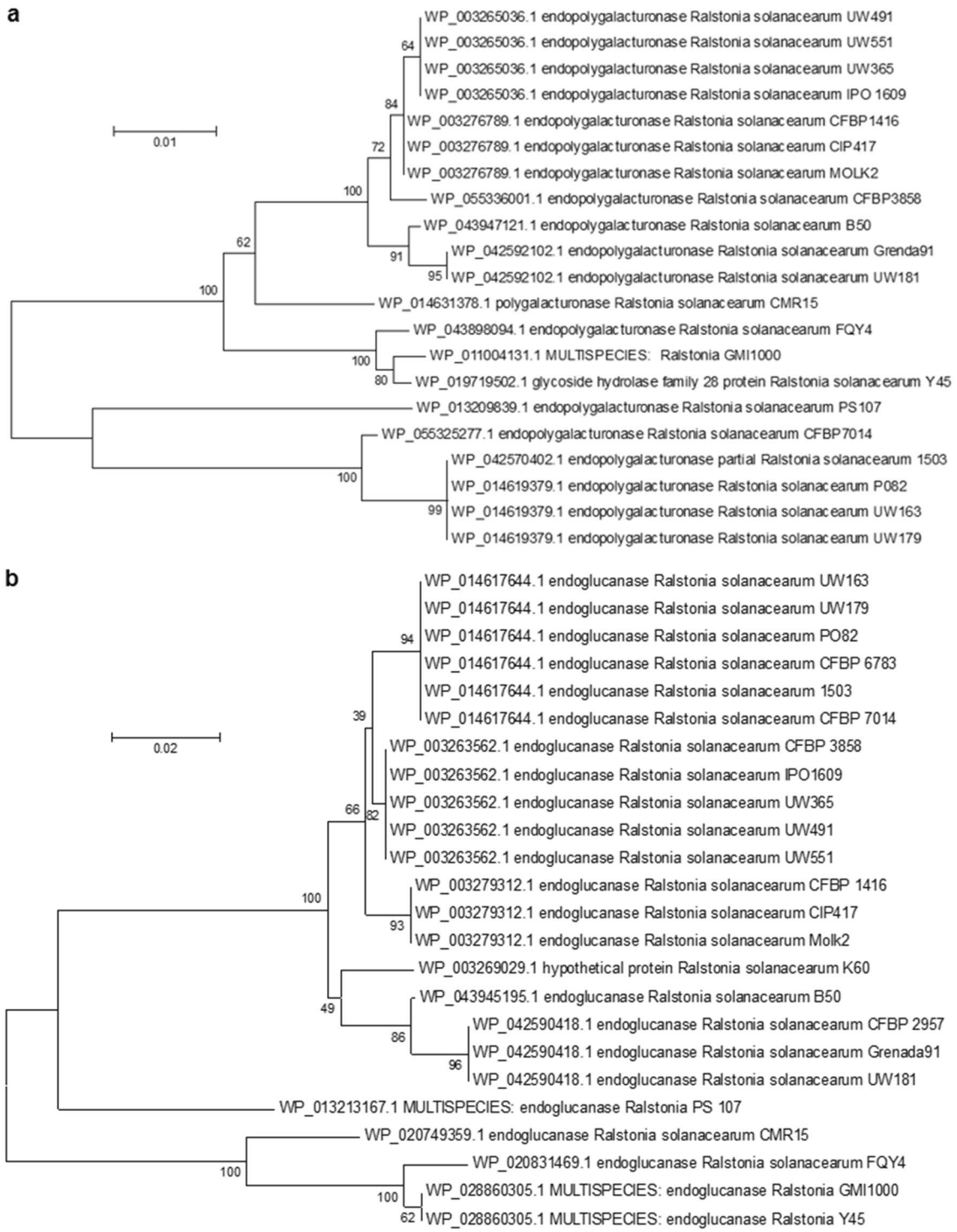

Fig. 1 Phylogenetic trees obtained for **a** *R. solanacearum* polygalacturonase and **b** *R. solanacearum* endoglucanase. The number of nodes in each tree represents the percentage of bootstrap values computed from 1000 re-samples. Bars indicate the substitutions occurring per amino acid position to reach the corresponding bacterial strain

Fig. 2c). The cellulose binding-like domain in this protein also demonstrates the features of PHL pollen allergen domains.

Physicochemical properties of the phytocompounds

The final set of ligands after filtration included 37 compounds, including 9, 20, 3, 5, and 8 from *C. sativum* L.,

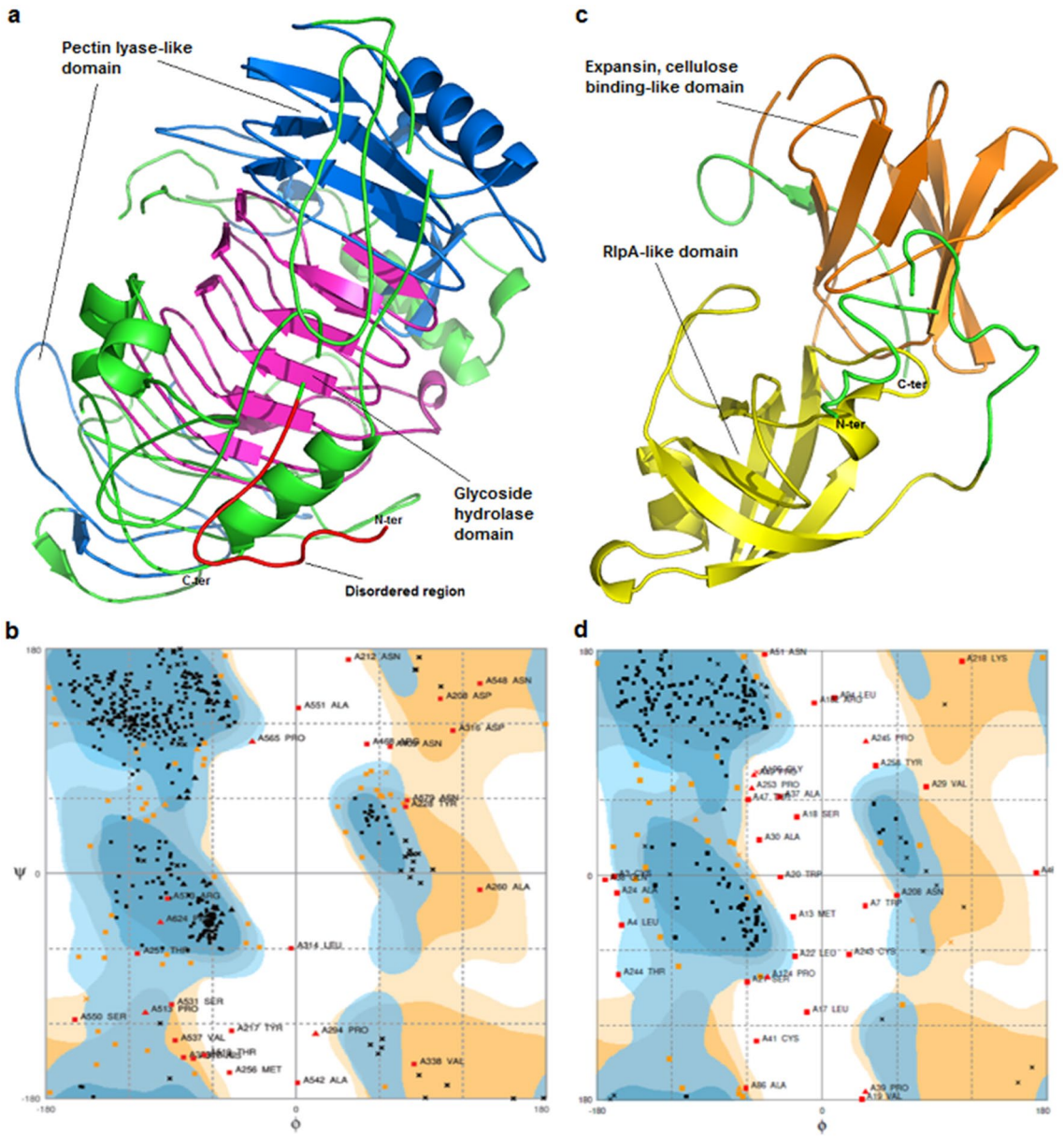

Fig. 2 Illustration and validation of the modeled three-dimensional structures of *R. solanacearum* polygalacturonase and endoglucanase. **a** Structure of polygalacturonase and its domains. Of note, the glycoside hydrolase domain acts also as a pectin lyase-like domain; **b** Ramachandran plot for the predicted model of polygalacturonase; **c** structure of endoglucanase and its domains. The expansin, cellulose binding-like domain acts also as a PHL pollen allergen domain; **d** Ramachandran plot for the predicted model of endoglucanase. Structures were rendered using Pymol (http://www.pymol.org)

C. citratus, *O. basilicum*, *R. officinalis* L., and *T. vulgaris*, respectively (summed not counting redundancies). The names list and the results of predicting the physicochemical properties and toxicity potential of these phytoligands are shown in Table 1. All the ligands demonstrated normal degrees of solubility in water and lipid phases. In addition, none of the studied molecules can inhibit cytochrome P450 isoforms; thus, they are predicted to be safe with no toxic effects to humans. The herbal compounds' ability to penetrate the skin was also predicted. With almost all the log K_p values being ≤ -4, the studied compounds can be classified as lowly probable to improbable to cross the skin.

Molecular docking

For each of the five herbal sources, the three compounds that showed the highest binding energy in docking with *R. solanacearum* proteins have been listed in Table 2 for

Table 1 Physicochemical properties and potential of toxicity calculated for the phytocompounds

Name (Accession)	Source	Lipophilicity (iLogP)	Water solubility		Pharmacokinetics	
			Log *S* (ESOL)	Class[a]	CYP inhibitor[b]	Log K_p (cm/s)[c]
(E)-β-Ocimene (5,281,553)	*C. citratus*	2.8	−3.17	S	No	−4.11
(Z)-β-Ocimene (5,320,250)	*C. citratus*	2.8	−3.17	S	No	−4.11
1-Decanol (8174)	*C. sativum*	2.99	−3.17	S	No	−4.02
3,7-Dimethyloct-1,5-dien-3,7-diol (5,352,451)	*O. basilicum*	2.47	−1.32	VS	No	−6.56
3,7-Dimethylocta-1,7-dien-3,6-diol (548,927)	*O. basilicum*	2.15	−1.66	VS	No	−6.10
3-Octanol (11,527)	*T. vulgaris*	2.55	−2.07	S	No	−5.12
6-Methyl-5-hepten-2-one (9862)	*C. citratus*	2.23	−1.61	VS	No	−5.73
Borneol (64,685)	*R. officinalis; C. citratus*	2.29	−2.51	S	No	−5.31
Camphor (2537)	*R. officinalis; C. citratus*	2.12	−2.16	S	No	−5.67
Carvone (7439)	*C. citratus*	2.27	−2.41	S	No	−5.29
Cineole (2758)	*R. officinalis*	2.58	−2.52	S	No	−5.30
Citronella (7794)	*C. citratus*	2.49	−2.88	S	No	−4.52
Citronellol (8842)	*C. citratus*	2.72	−2.94	S	No	−4.48
Citronellyl acetate (9017)	*C. citratus*	3.29	−3.43	S	No	−4.33
Cyclohexane (8078)	*T. vulgaris*	2.1	−2.53	S	No	−4.37
Decanal (8175)	*C. sativum*	2.72	−2.67	S	No	−4.56
Decane (15,600)	*C. sativum*	3.29	−3.42	S	No	−3.61
Dodecanoic acid (3893)	*C. sativum*	2.7	−3.07	S	No	−4.54
Endo-borneol (1,201,518)	*T. vulgaris*	2.29	−2.51	S	No	−5.31
Geranial (638,011)	*O. basilicum; C. citratus*	2.47	−2.43	S	No	−5.08
Geraniol (637,566)	*C. citratus; O. bacilicum*	2.75	−2.78	S	No	−4.71
Geranyl acetate (1,549,026)	*C. citratus; O. bacilicum*	2.83	−3.21	S	No	−4.63
Linalool (6549)	*T. vulgaris; C. citratus; C. Sativum*	2.7	−2.4	S	No	−5.13
β-Myrcene (31,253)	*R. officinalis; C. citratus; T. vulgaris*	2.89	−3.05	S	No	−4.17
Neral (643,779)	*C. citratus*	2.47	−2.43	S	No	−5.08
Nerol (643,820)	*O. bacilicum*	2.75	−−2.78	S	No	−4.71
n-Nonanol (8914)	*C. sativum*	2.72	−2.65	S	No	−4.50
n-Octyl acetate (8164)	*O. bacilicum*	2.8	−2.53	S	No	−4.93
Nonanal (31,289)	*C. sativum*	2.44	−2.31	S	No	−4.85
Nonane (8141)	*C. sativum*	3.06	−3.8	S	No	−3.07
Octanal (454)	*C. sativum*	2.29	−1.95	VS	No	−5.15
Piperitone (6987)	*C. citratus*	2.38	−2.51	S	No	−5.21
Sabinene (18,818)	*C. citratus*	2.65	−2.57	S	No	−4.94
Terpinen-4-ol (11,230)	*C. citratus; T. vulgaris*	2.51	−2.78	S	No	−4.93
γ-Terpinene (7461)	*T. vulgaris*	2.73	−3.45	S	No	−3.94
α-Terpineol (17,100)	*R. officinalis; C. citratus; T. vulgaris*	2.51	−2.87	S	No	−4.83
Tricyclene (79,035)	*C. citratus*	2.53	−2.73	S	No	−4.83

PG and Table 3 for EG. Interaction diagrams showing the hydrophobic interactions and hydrogen bonds of all the ligands with the two proteins were drawn and shown for PG in the Online Resource 1 Table S1, and for EG in the Online Resource 1 Table S2. As a general rule, ligands having more –CH2– groups (aliphatic hydrocarbon) or double bonds or an aromatic ring in their structure were surrounded by a large number of hydrophobic residues and had higher affinity to bind PG or EG, compared to those without such groups. This feature indicates the important contribution of hydrophobic forces in shaping and stabilizing the interactions of PG and EG with their corresponding ligands. In

Table 2 The binding energy and the interactions for top three best binding phytoligands from each of the sources, for binding to polygalacturonase

Source	Compound	Binding energy (kcal/mol)	Inhibition constant (K_i; μM)	Interacting amino acids
O. basilicum	3,7-Dimethylocta-1,7-dien-3,6-diol	−5.09	184.49	I395, S292, A290, F480, A482, T483, V282, A281, Y481, S451
	Geranyl acetate	−5.25	142.32	G280, G420, V282, Y481, E278, A482, S451, F480, T483, S292, I395
	3,7-Dimethylocta-1,5-dien-3,7-diol	−5.27	137.26	V282, A482, Y481, T483, F480, S451, A290, S292, I395
C. sativum	Linalool	−5.03	205.25	T483, P294, A281, V282, S292, F480, T419, G452, S451, I395, G420, Y481, A482
	Decanal	−3.85	1510.0	V282, S292, G396, F480, A482, Y481, T483, I395, Y279, E278, G280, W270
	Nonanal	−3.84	1540.0	G396, I395, V282, T483, A482, F480, S292, Y481, Y279, G280, E278, W270
C. citratus	α-Terpineol	−5.58	81.83	E278, V282, S292, I395, G420, F480, Y481, A482, T483
	Terpinen-4-ol	−5.46	99.48	A281, V282, S292, I395, F480, Y481,A482, T483
	Carvone	−5.66	70.7	V282, S292, I395,T419, G420, S451, G452, F480, Y481, A482, T483
R. officinalis	α-Terpineol	−5.58	81.83	E278, V282, S292, I395, G420, F480, Y481, A482, T483
	Borneol	−5.14	171.53	F480, N514, A551, R553, G642, P643, A644
	Camphor	−5.05	200.28	F480, N514, A551, R553, G642, P643, A644
T. vulgaris	Terpinen-4-ol	−5.46	99.48	A482, I395, F480, A281, Y481, V282, T483, S292
	α-Terpineol	−5.58	81.83	A482, S292, F480, V282, G420, E278, I395, Y481, T483
	Endo-borneol	−5.14	170.11	R553, A644, P643, N514, G642, F480

Table 3 The binding energy and the interactions for top three best binding phytoligands from each of the sources, for binding to endoglucanase

Source	Compound	Binding energy (kcal/mol)	Inhibition constant (K_i; μM)	Interacting amino acids
O. basilicum	Geraniol	−4.61	419.05	H23, S16, M13, L14, W7, L122, L15, D206, Y207
	Nerol	−4.52	485.17	H23, Y207, D206, M13, L122, W7, L14, L15, S16
	Geranyl acetate	−4.92	249.38	M13, P89, P124, W7, C3, R8, A127, A90, A126, S128, E125, L4, L122
C. sativum	Linalool	−4.58	439.69	A126, L4, P89, E125, R8, P124, C3, W7, A90
	Dodecanoic acid	−4.65	391.13	L22, H23, K204, A205, V211, V28, P23, G212, V200, L215, T213, N25, A24
	N-nonanol	−4.47	525.45	P124, R8, W7, A90, A126, L122, M13, C3, P89, E125
C. citratus	Piperitone	−5.18	160.0	F57, A50, Q91, A90, L42, G95, L94, T47
	α-Terpineol	−5.09	184.46	A126, A127, N88, S128, L4, R8, C3, E125, P89, A90
	Citronellyl acetate	−5.23	147.55	A126, N88, A127, A90, S128, P88, L122, P124, M13, W7, R8, C3, L4, E125
R. officinalis	Cineole	−4.89	261.65	H23, V211, A25, P203, T213, V28, A24, L22
	Borneol	−4.94	240.91	D206, S16, W7, M13, L14, L15, Y207
	α-Terpineol	−5.09	184.46	A126, A127, N88, S128, L4, R8, C3, E125, P89, A90
T. vulgaris	Endo-borneol	−4.84	285.43	K169, E170, G171, S172, A178, W176, A177
	Terpinen-4-ol	−4.77	319.07	L15, D206, Y207, S16, W7, L14, M13
	α-Terpineol	−5.09	184.46	A126, N88, A127, S128, L4, R8, C3, E125, P89, A90

Fig. 3, all the binding energies have been illustrated as a graphical heatmap. On average, compounds from *C. citratus* and *T. vulgaris* had more favorable binding to PG, and compounds from *C. sativum* showed a weak binding (Table 2). The binding of the compounds to EG was generally weaker than their interactions with PG. Phytoligands from *C. citratus* and *R. officinalis* demonstrated the best interactions with EG (Table 3).

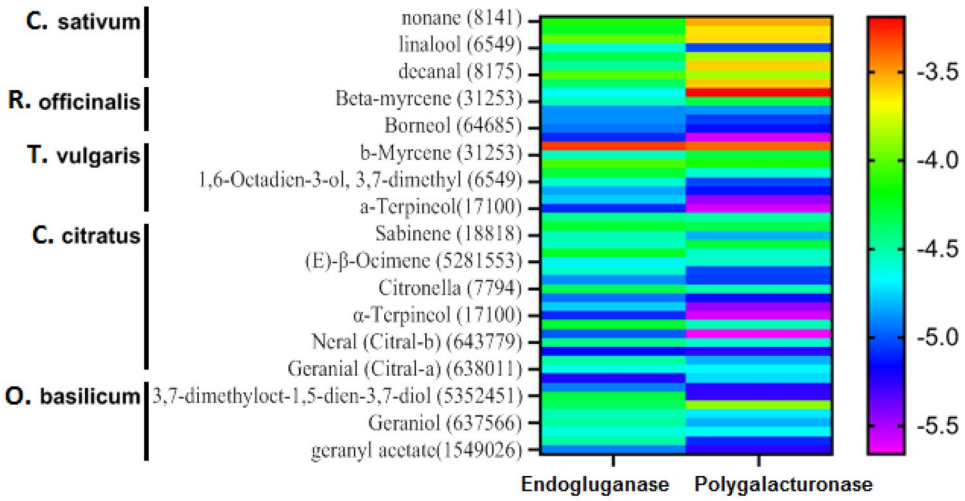

Fig. 3 Heat map of the energies (kcal/mol^{-1}) obtained in molecular docking of phytoligands to *R. solanacearum* polygalacturonase and endoglucanase

Carvone (7439) from *C. citratus* was predicted as the best inhibitor of PG, with an energy of binding of -5.66 kcal/mol and an inhibition constant (K_i) of 70.7 µM. The main residues involving in the PG-Carvone interaction were Thr483, Ala482, Phe480, Ser451, Thr419, Tyr481, Gly452, Gly420, Ile395, Val282, and Ser292.

Furthermore, Citronellyl acetate (9017) from *C. citratus* showed an energy of −5.23 kcal/mol and the predicted K_i of 147.55, and was known as the best inhibitor of EG. Important amino acids contributing to the interaction of Citronellyl acetate with EG were Ala126, Asn88, Ala127, Ala90, Ser128, Pro88, Leu122, Pro124, Met13, Trp7, Arg8, Cys3, Leu4, and Glu125.

Molecular dynamics simulations

RMSD and RMSF were referred to as the measures to assess the dynamic behavior of the best phytoligand–protein complexes, i.e., Carvone-PG and citronellyl acetate-EG. The general deviation of structure along the simulation time compared to the initial timepoint is shown using the RMSD plot. Small slopes imply a stable model. Carbon α-RMSDs in the studied ligand–protein systems are displayed in Figs. 4A and 5A for Carvone-PG and citronellyl acetate-EG complexes, respectively. The trends for both proteins indicate roughly smooth dynamics along the simulation, specifically when comparing the ligand-bound and ligand-free states. This observation points toward the high stability of the protein structures when bound to their corresponding ligands.

Atomic RMSDs for each respective ligand are displayed in Figs. 4B and 5B. This plot is aimed to indicate whether the ligand remains stable in the protein's binding site. As can be observed, the phytoligand carvone bound to PG jumps from RMS = 0.05 nm to 0.13 nm at t of 7.31 ns, but it stays almost smooth through to the final point (Fig. 4B). Apart from this drift in PG's binding site, the ligand RMSD trends indicate the stable binding of both ligands in their respective binding cavities.

The RMSF measure is aimed to depict the local residual oscillation along the simulated protein's sequence. Limited residue fluctuation in this plot can be associated with the protein–ligand's physical interaction; amino acids composing the binding site are usually less flexible than other parts, mainly owing to the ligand's binding. Figures 4C and 5C illustrate the RMSF plots for PG and EG, respectively. Considering the residual composition of the binding sites of the two proteins, the amino acids participating in the interaction with the phytoligands are observed to show limited mobility and fluctuate the least. Thus, the interactions occurring at the receptor–ligand interface are concluded to be stable in general. In both plots, there are regions with high RMSF values. These include residues 35, 66, 92, 122, and 290 on the PG's RMSF plot, and residues 4, 42, and 250 of EG. Our visual inspection of the structures showed that all these regions compose the loops or terminal parts of these proteins. Taking into consideration the above-mentioned locations of domains and the binding sites of PG and EG, we can see that none of these highly flexible regions locate in the functional domains or in the binding sites of either of the two proteins. Thus, they may not affect the stability of ligand binding in PG and EG.

The count of inter-molecular hydrogen bonds is used as another measure of stability for ligand–protein systems. By examining the H-bond diagrams for the simulated systems in the current study (Figs. 4D and 5D), it was seen that these bonds form, disappear, re-form, and persist continuously over time. For EG-citronellyl acetate, the bonds increase and maintain. It is noteworthy that hydrophobic and electrostatic interactions also contribute to any ligand-receptor binding. Thus, the found H-bonds, combined with other types of interactions, will lead to a preserved ligand–protein complex for the *R. solanacearum* enzymes studied here. Dynamic

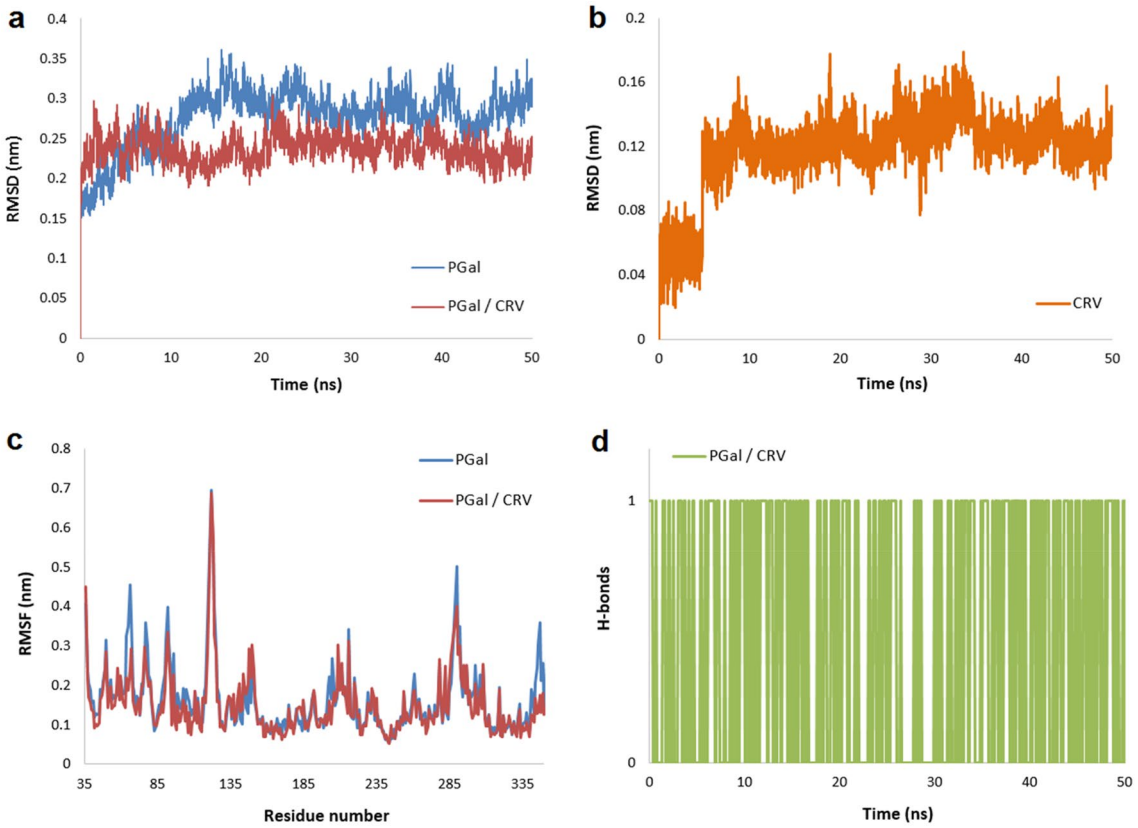

Fig. 4 MD simulation analysis of *R. solanacearum* polygalacturonase (PGal) bound to Carvone (CRV). **a** Root-mean-square deviation (RMSD) plot for the ligand-bound and free protein; **b** ligand's RMSD plot; **c** root-mean-square fluctuations (RMSF) plot for the ligand-bound and free protein; **d** the count of hydrogen bonds between the ligand and the protein along the time

plots showed that the count and the energy of the bonds were sufficient to keep the ligand firm at the two enzymes' binding sites.

Discussion

Interest is growing nowadays toward assaying for phytochemicals as natural antimicrobial agents against plant pathogens (Mahomoodally et al. 2005). In recent years, the antibacterial effects of various plants have been extensively reported (Nascimento et al. 2000). Plants are known to have an almost unlimited capability to produce aromatic compounds, mostly phenols and their derivatives with oxygen substitution. In numerous cases, the compounds serve as defense mechanisms for the plant against predation by microorganisms (Cowan 1999).

Computer-aided drug design (CADD) has been used extensively in pharmaceutical industries, with some applications in the area of herbal disease (Taylor 2016; Singh et al. 2020; Kumar et al. 2023; Singh and Purohit 2023). Using CADD, Yang et al (2002) showed that the novel 2-heteroaryl-4-chromanones can be more effective in fight with rice blast fungus (*Magnaporthe grisea*). Zhou et al. (Zhou et al. 2015) applied molecular docking to predict how eight mutants of *Peronophythora litchii* modify the interaction between novel QoI-type fungicides and the Qo-binding cavities. Omar et al. (2021) examined the leaf extract of *Olea europaea*, and the essential oils of *Boswellia carteri* and *T. vulgaris* as prospective candidates for fungal inhibition by anti-fungal evaluation and molecular docking. However, the CADD techniques have not been broadly applied in designing or developing chemical ligands able to treat crop plants' diseases. In this study, the molecular docking and MD simulations were carried out to examine the binding interactions of 37 phytocompounds from five medicinal plants (*R. officinalis L.*, *C. sativum L.*, *O. basilicum*, *C. citratus*, and *T. vulgaris*) with the binding pocket of PG and EG of R. solanacearum.

Extracellular proteins that degrade the plant cell walls are known as key virulence factors contributing to the appearance of bacterial wilt symptoms (Schacht et al. 2011). PG and EG have been shown to play a marked role in the infection processes and cell wall degradation. Our study identified carvone and citronellyl acetate as the best inhibitors against *R. solanacearum* PG and EG, respectively. Dynamic

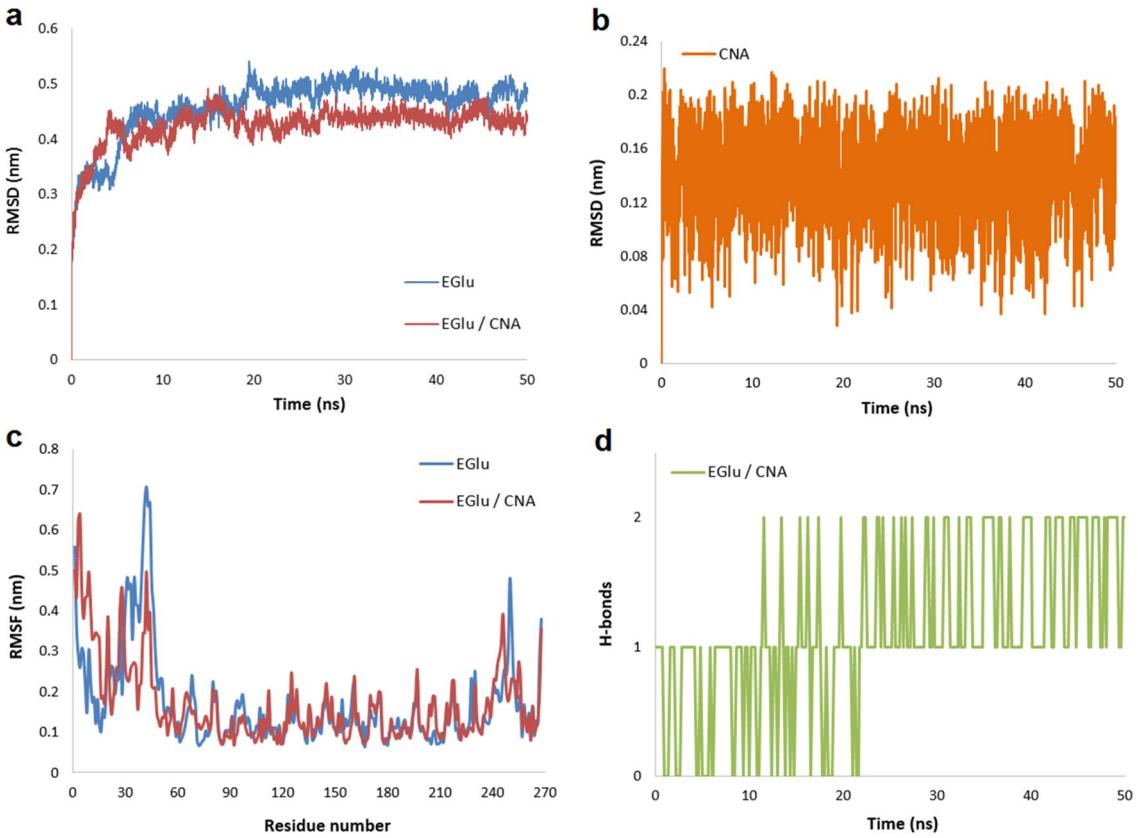

Fig. 5 MD simulation analysis of *R. solanacearum* endoglucanase (EGlu) bound to Citronellyl acetate (CNA). **a** Root-mean-square deviation (RMSD) plot for the ligand-bound and free protein; **b** ligand's RMSD plot; **c** root-mean-square fluctuations (RMSF) plot for the ligand-bound and free protein; **d** the count of hydrogen bonds between the ligand and the protein along the time

simulations confirmed the high stability of these ligands at the active site of PG and EG.

In agreement with the PG inhibitory effect of carvone, the study by Paret et al (2010) revealed the bactericidal ability of lemongrass on race-4 *R. solanacearum*, a strain causing bacterial wilts on tomato and ginger in some regions of the world. Various highly abundant herbal compounds, such as terpenoids, are appreciated as active inhibitors against a wide variety of pathogens (Trombetta et al. 2005). Monoterpenes, such as thymol, carvacrol, geraniol, and menthol, can act against Gram-positive and Gram-negative bacteria. Geraniol, a potent efflux pump inhibitor, was reported to effectively augment the susceptibility in the multi-drug resistant Gram-negative bacterium *Enterobacter aerogenes* (Lorenzi et al. 2009). Phenol monoterpenes, like carvacrol, were also demonstrated to prevent biofilm development of *S. typhimurium* and *S. aureus* (Knowles et al. 2005). As shown by the docking results of our study, it seems that the non-polar energy component contributed by aliphatic groups on these molecules may serve as a critical driving force in their mechanism of inhibition on the *R. solanacearum* PG.

Citronellyl acetate, the identified inhibitor for EG, is a monoterpenoid that is the acetate ester of citronellol. Terpenoids, which are derivatives of terpenes, have been proven active against bacteria (Nazzaro et al. 2013). Carvacrol, menthol, thymol, linalool, geraniol, piperitone, citronella, and linalyl acetrate are some of the most potent and widely studied terpenoids (Mahizan et al. 2019). Terpenoids' antimicrobial activity is decided from the functional groups on them. The main antimicrobial determining factors include the hydroxyl group of the phenolic terpenoids and delocalized electrons (Griffin et al. 1999). Consistently, our MD results confirmed the contribution of the –OH group of citronellyl acetate in forming hydrogen bonds with residues of EG. Nonpolar interactions were also shown to play a significant role in shaping the interaction. Although the exact mode of action of terpenoids remains unclarified, Griffin et al (1999) showed that most terpenoids can prevent oxidative phosphorylation and oxygen uptake, two vital processes which are important to microbial survival. Interestingly, our results also identified the terpenoid α-Terpineol from various sources as one of the strong ligands against both PG and EG.

Conclusion

The present study involved applying in silico CADD techniques, including molecular docking and molecular dynamic simulations, to examine the potential of phytoligands from five herbal sources to inhibit PG and EG of *R. solanacearum*, the causing agent of wilts. In addition to favorable pharmacokinetic profiles, the binding analyses using docking affinity and solution dynamics were also promising and confirmed each other. Carvone was identified as a potential lead against PG, and citronellyl acetate showed great inhibitory potential against EG.

Practical experimental studies are required to verify the efficacy and specificity of the introduced natural organics. Such corroborations would inform future research to use these phytomolecules for investigating more potent pesticides or antibacterials through ligand-based screening or pharmacophore modeling. Further validations in vivo would then be necessary to reach a final formula; however, there would be no public concern or regulatory issue in terms of safety, off-targets, and environment friendliness, as the compounds are derived from edible plants. Such considerations, in turn, will allow the integrating of the final identified phytocompounds into appropriate formulations to be introduced to the market.

Exploring natural products as possible bactericidal agents and applying CADD methods as primary, low-cost, and less time-consuming techniques to achieve this aim are the main implications of this study. Other widespread crop pathogens can be targeted using the same approach adopted in this research. Furthermore, as both best-energy compounds were from lemongrass (*C. citratus*), this plant may have the potential for suppressing similar pathogens affecting agriculturally important species other than crops.

Supplementary Information The online version contains supplementary material available at https://doi.org/10.1007/s13205-023-03683-z.

Author contributions FE contributed to conceptualization, formal analysis and investigation, original draft writing, and preparation; EB contributed to methodology, formal analysis and investigation, manuscript review and editing, resources, and supervision.

Funding No funding was received for conducting this study.

Data transparency The authors declare that all data and materials as well as software application or custom code used in this study support their published claims and comply with the field standards.

Declarations

Conflict of interest The authors declare that they have no conflict of interest in the publication.

Research involving human participants and/or animals This research did not involve any human participants and/or animals on which experiments could be conducted.

Informed consent This research did not involve any human participants whose consents could be taken for publication of this research-related data.

References

Abd-Elrahim R, Tohamy MRA, Atia MM, Elashtokhy MMA, Ali MAS (2022) Bactericidal activity of some plant essential oils against *Ralstonia solanacearum* infection. Saudi J Biol Sci 29(4):2163–2172

Adam M (2005) Integrating research and development: the emergence of rational drug design in the pharmaceutical industry. Stud Hist Philos Biomed Sci 36:513–537

Aliye M, Dekebo A, Tesso H, Abdo T, Eswaramoorthy R, Melaku Y (2021) Molecular docking analysis and evaluation of the antibacterial and antioxidant activities of the constituents of *Ocimum cufodontii*. Sci Rep 11:10101. https://doi.org/10.1038/s41598-021-89557-x

Alsaraf S, Hadi Z, Al-Lawati WM, Al Lawati AA, Khan SA (2020) Chemical composition, *in vitro* antibacterial and antioxidant potential of *Omani Thyme* essential oil along with in silico studies of its major constituent. J King Saud Univ Sci 32(1):1021–1028

Andrade JM, Faustino C, Garcia C, Ladeiras D, Reis CP, Rijo P (2018) *Rosmarinus officinalis* L.: an update review of its phytochemistry and biological activity. Fut Sci 4(4):283. https://doi.org/10.4155/fsoa-2017-0124

Araújo Silva V, Pereira da Sousa J, de Luna Freire Pessôa H, Fernanda Ramos de Freitas A, Douglas Melocoutinho H, Beuttenmuller Nogueiraalves L, Oliveiralima E (2016) *Ocimum basilicum*: Antibacterial activity and association study with antibiotics against bacteria of clinical importance. Pharm Biol 54(5):863–867. https://doi.org/10.3109/13880209.2015.1088551

Bassolé IHN, Lamien-Meda A, Bayala B, Tirogo S, Franz CH, Novak J, Charles Nebie R, Hama Dicko M (2010) Composition and antimicrobial activities of *Lippia multiflora moldenke, mentha* × *piperita l and Ocimum basilicum* L. essential oils and their major monoterpene alcohols alone and in combination. Molecules 3(15):7825–7839

Bozin B, Mimica-Dukic N, Samojlik I, Jovin E (2007) Antimicrobial and antioxidant properties of rosemary and sage (*Rosmarinus officinalis* L. and *Salvia officinalis* L., Lamiaceae) essential oils. J Agric Food Chem 55:7879–7885. https://doi.org/10.1021/jf071515323

Bussi G, Donadio D, Parrinello M (2007) Canonical sampling through velocity rescaling. J Chem Phys 126:014101. https://doi.org/10.1063/1.2408420

Cho H, Song ES, Heu S, Baek J, Lee YK, Lee S, Lee SW, Park DS, Lee TH, Kim JG, Hwang I (2019) Prediction of host-specific genes by pan-genome analyses of the Korean *Ralstonia solanacearum* species complex. Front Microbiol 15(10):506. https://doi.org/10.3389/fmicb.2019.00506

Cowan MM (1999) Plant products as antimicrobial agents. Clin Microbiol Rev 12(4):564–582. https://doi.org/10.1128/CMR.12(4):564-582

Daferera DJ, Ziogas BN, Polissiou MG (2003) The effectiveness of plant essential oils in the growth of *Botrytis cinerea*, Fusarium sp. and *Clavibacter michiganensis* subsp. *michiganensis*. Crop Protec 22(1):39–44

Daina A, Michielin O, Zoete V (2017) Swiss ADME: a free web tool to evaluate pharmacokinetics, drug-likeness and medicinal chemistry friendliness of small molecules. Sci Rep 7:42717. https://doi.org/10.1038/srep42717

Darden T, York D, Pedersen L (1993) Particle mesh Ewald: An N·log(N) method for Ewald sums in large systems. J Chem Phys 98:10089–10092. https://doi.org/10.1063/1.464397

Genin S, Denny TP (2012) Pathogenomics of the *Ralstonia solanacearum* species complex. Annu Rev Phytopathol 50:67–89

Grey BE, Steck TR (2001) The viable but nonculturable state of *Ralstonia solanacearum* may be involved in long-term survival and plant infection. Appl Environ Microbiol 67(9):3866–3872

Griffin SG, Wyllie SG, Markham JL, Leach DN (1999) The role of structure and molecular properties of terpenoids in determining their antimicrobial activity. Flavour Fragr J 14(5):322–332. https://doi.org/10.1002/(SICI)1099-1026(199909/10)14:5%3c322::AID-FFJ837%3e3.0.CO;2-4

Hess B, Bekker H, Berendsen HJC, Fraaije JGEM (1998) LINCS: A linear constraint solver for molecular simulations. J Computational Chem 18(12):1463–1472. https://doi.org/10.1002/(sici)1096-987x(199709)18:12%3c1463::aid-jcc4%3e3.0.co;2-h

Hong JC, Momol MT, Ji P, Olson SM, Colee J, Jones JB (2011) Management of bacterial wilt in tomatoes with thymol and acibenzolar-S-methyl. Crop Prot 30(10):1340–1345

Kim S, Chen J, Cheng T, Gindulyte A, He J, Li Q, Shoemakr BA, Thiessen PA, Yu B, Zaslavsky L, Zhang J, Bolton E (2020) PubChem in 2021: new data content and improved web interfaces. Nucleic Acids Res 49(D1):D1388–D1395. https://doi.org/10.1093/nar/gkaa971

Kimura M (1980) A simple method for estimating evolutionary rates of base substitutions through comparative studies of nucleotide sequences. J Mol Evol 16(2):111–120

Knowles JR, Roller S, Murray DB, Naidu AS (2005) Antimicrobial action of carvacrol at different stages of dual-species biofilm development by *Staphylococcus aureus* and *Salmonella enterica* serovar typhimurium. Appl Environ Microbiol 71(2):797–803. https://doi.org/10.1128/AEM.71.2.797-803.2005

Kong HG, Bae JY, Lee HJ, Joo HJ, Jung EJ, Chung E, Lee SW (2014) Induction of the viable but nonculturable state of *Ralstonia solanacearum* by low temperature in the soil microcosm and its resuscitation by catalase. PLoS ONE 9:e109792

Kozakov D, Grove LE, Hall DR, Bohnuud T, Mottarella SE, Luo L, Xia B, Beglov D, Vajda S (2015) The FTMap family of web servers for determining and characterizing ligand-binding hot spots of proteins. Nat Protoc 10(5):733–755

Kumar S, Bhardwaj VK, Singh R, Purohit R (2023) Structure restoration and aggregate inhibition of V30M mutant transthyretin protein by potential quinoline molecules. Int J Biol Macromol 231:123318. https://doi.org/10.1016/j.ijbiomac.2023.123318

Liu H, Zhang S, Schell MA, Denny TP (2005) Pyramiding unmarked deletions in *Ralstonia solanacearum* shows that secreted proteins in addition to plant cell-wall-degrading enzymes contribute to virulence. Mol Plant Microbe Interact 18(12):1296–1305

Lo Cantore P, Iacobellis NS, De Marco A, Capasso F, Senatore F (2004) Antibacterial activity of *Coriandrum sativum* L. and *Foeniculum vulgare* Miller Var. vulgare (Miller) essential oils. J Agri Food Chem 52:7862–7866

Lorenzi V, Muselli A, Bernardini AF, Berti L, Pages JM, Amaral L, Bolla JL (2009) Geraniol restores antibiotic activities against multidrug-resistant isolates from Gram-negative species. Antimicrob Agent Chemother 53:2209–2211. https://doi.org/10.1128/AAC.00919-08

Mahizan NA, Yang SK, Moo CL, Song AA, Chong CM, Chong CW, Abushelaibi A, Lim SE, Lai KS (2019) Terpene Derivatives as a Potential Agent against Antimicrobial Resistance (AMR) Pathogens. Molecules 19:24(14):2631. https://doi.org/10.3390/molecules24142631

Mahomoodally MF, Gurib-Fakim A, Subratty AH (2005) Antimicrobial activities and phytochemical profiles of endemic medicinal plants of mauritius. Pharm Biol 43(3):237–242. https://doi.org/10.1080/13880200590928825

Malde AK, Zuo L, Breeze M, Stroet M, Poger D, Nair PC, Oostenbrink C, Mark AE (2011) An automated force field topology builder (ATB) and repository. J Chem Theory Comput 7(12):4026–4037. https://doi.org/10.1021/ct200196m

Martonák R, Laio A, Parrinello M (2003) Predicting crystal structures: the Parrinello-Rahman method revisited. Phys Rev Lett 90(7):075503. https://doi.org/10.1103/PhysRevLett.90.075503

Morris GM, Huey R, Lindstrom W, Sanner MF, Belew RK, Goodsell DS, Olson AJ (2009) Autodock4 and AutoDockTools4: automated docking with selective receptor flexiblity. J Comput Chem 16:2785–2791

Nascimento GGF, Locatelli J, Freitas PC, Silva G (2000) Antibacterial activity of plant extracts and phytochemicals on antibiotic-resistant bacteria. Braz J Microbiol 31(4):247–256

Nazzaro F, Fratianni F, De Martino L, Coppola R, De Feo V (2013) Effect of essential oils on pathogenic bacteria. Pharmaceuticals 6:1451–1474. https://doi.org/10.3390/ph6121451

Omar HS, Abd El-Rahman SN, AlGhannam ShM, Reyad NEH, Sedeek MS (2021) Antifungal evaluation and molecular docking studies of *Olea europaea* leaf extract, *Thymus vulgaris* and *Boswellia carteri* essential oil as prospective fungal inhibitor candidates. Molecules 26(20):6118. https://doi.org/10.3390/molecules26206118.Erratum.In:Molecules(2022)27(12)

Palacio-Bielsa A, Cambra MA, López MM (2009) PCR detection and identification of plant-pathogenic bacteria: updated review of protocols 1989–2007. J Plant Pathol 91(2):912–957

Paret ML, Cabos R, Kratky BA, Alvarez AM (2010) Effect of plant essential oils on *Ralstonia solanacearum* race 4 and bacterial wilt of edible ginger. Plant Dis 94(5):521–527

Pathak RK, Taj G, Pandey D, Kasana VK, Baunthiyal M, Kumar A (2016) Molecular modeling and docking studies of phytoalexin(s) with pathogenic protein(s) as molecular targets for designing the derivatives with anti-fungal action on '*Alternaria*' spp. of '*Brassica*'. Plant Omics J 9:172–182

Paysan-Lafosse T, Blum M, Chuguransky S, Grego T, Pinto BL, Salazar GA, Bileschi ML, Bork P, Bridge A, Colwell L, Gough J, Haft DH, Letunić I, Marchler-Bauer A, Mi H, Natale DA, Orengo CA, Pandurangan AP, Rivoire C, Sigrist CJA, Sillitoe I, Thanki N, Thomas PD, Tosatto SCE, Wu CH, Bateman A (2023) InterPro in 2022. Nucl Acids Res 51(D1):D418–D427. https://doi.org/10.1093/nar/gkac993

Pronk S, Páll S, Schulz R, Larsson P, Bjelkmar P, Apostolov R, Shirts MR, Smith JC, Kasson PM, van der Spoel D, Hess B, Lindahl E (2013) GROMACS 4.5: a high-throughput and highly parallel open source molecular simulation toolkit. Bioinformatics (Oxford, England) 29(7):845–854. https://doi.org/10.1093/bioinformatics/btt055

Raza W, Ling N, Yang L, Huang Q, Shen Q (2016) Response of tomato wilt pathogen *Ralstonia solanacearum* to the volatile organic compounds produced by a bio control strain *Bacillus amyloliquefaciens* SQR-9. Sci Rep 6:24856

Reddy P, Kandisa RV, Varsha P, Satyam S (2014) Review on *Thymus vulgar*is traditional uses and pharma- cological properties. Med Aromat Plants 3(3):164

Saitou N, Nei M (1987) the neighbor-joining method: a new method for reconstructing phylogenetic trees. Mol Biol Evol 4(4):406–425. https://doi.org/10.1093/oxfordjournals.molbev.a040454

Schacht T, Unger C, Pich A, Wydra K (2011) Endo- and exopolygalacturonases of *Ralstonia solanacearum* are inhibited by polygalacturonase-inhibiting protein (PGIP) activity in tomato stem extracts. Plant Physiol Biochem 49(4):377–387

Schweitzer B, Balázs VL, Molnár S, Szögi-Tatár B, Böszörményi A, Palkovics T, Horváth G, Schneider G (2022) Antibacterial Effect of Lemongrass (*Cymbopogon citratus*) against the Aetiological

Agents of Pitted Keratolyis. Molecules 27(4):1423. https://doi.org/10.3390/molecules27041423
Selvam K, Senbagam D, Selvankumar T, Sudhakar C, Kamala-Kannan S, Senthilkumar B, Govarthanan M (2017) Cellulase enzyme: Homology modeling, binding site identification and molecular docking. J Mol Struct 1150:61–67. https://doi.org/10.1016/j.molstruc.2017.08.067
Singh R, Purohit R (2023) Computational analysis of protein–ligand interaction by targeting a cell cycle restrainer. Comput Methods Programs Biomed 231:107367. https://doi.org/10.1016/j.cmpb.2023.107367
Singh R, Bhardwaj VK, Sharma J, Purohit R (2020) Identification of novel and selective agonists for ABA receptor PYL3. Plant Physiol Biochem 154:387–395. https://doi.org/10.1016/j.plaphy.2020.05.005
Singh R, Bhardwaj VK, Das P, Purohit R (2021) New ecdysone receptor agonists: a computational approach for rational discovery of insecticides for crop protection. Mol Syst Des Eng 6:936–945. https://doi.org/10.1039/D1ME00047K
Stroet M, Caron B, Visscher KM, Geerke DP, Malde AK, Mark AE (2018) Automated topology builder Version 3.0: prediction of solvation free enthalpies in water and hexane. J Chem Theory Comput 14(11):5834–5845. https://doi.org/10.1021/acs.jctc.8b00768
Tamura K, Stecher G, Peterson D, Filipski A, Kumar S (2013) MEGA6: molecular evolutionary genetics analysis version 6.0. Mol Biol Evol 30(12):2725–2729
Taylor D (2016) The pharmaceutical industry and the future of drug development. In: Hester RE, Harrison RM (eds) Pharmaceuticals in the environment. The Royal Society of Chemistry, pp 1–33
Thompson JD, Higgins DG, Gibson TJ (1994) Clustalw: improving the sensitivity of progressive multiple sequence alignment through sequence weighting, position-specific gap penalties and weight matrix choice. Nucleic Acids Res 22(22):4673–4680. https://doi.org/10.1093/nar/22.22.4673
Trombetta D, Castelli F, Sarpietro MG, Venuti V, Cristani M, Daniele C, Saija A, Mazzanti G, Bisignano G (2005) Mechanisms of antibacterial action of three monoterpenes. Antimicrob Agents Chemother 49(6):2474–2478. https://doi.org/10.1128/AAC.49.6.2474-2478.2005
Van Overbeek LS, Bergervoet JHH, Jacobs FHH, van Elsas JDV (2004) The low-temperature-induced viable-but-nonculturable state affects the virulence of *Ralstonia solanacearum* biovar 2. Phytopathology 94(5):463–469
Wallace AC, Laskowski RA, Thornton JM (1995) Ligplot: A program to generate schematic diagrams of protein–ligand interactions. Prot Eng Des Sel 8(2):127–134. https://doi.org/10.1093/protein/8.2.127
Yang GF, Jiang XH, Yang DY, HZ, (2002) Three dimensional quantitative structure-activity relationships of novel 2-heteroaryl-4-chromanone derivatives. Acta Chim Sin 60:134–138
Zhou Y, Chen L, Hu J, Duan H, Lin D, Liu P, Meng Q, Li B, Si N, Liu C, Liu X (2015) Resistance mechanisms and molecular docking studies of four novel QoI fungicides in *Peronophythora litchii*. Sci Rep 5:17466. https://doi.org/10.1038/srep17466